

Targeted Polypeptide–Microtubule Aggregation with Cucurbit[8]uril for Enhanced Cell Apoptosis

Ying-Ming Zhang, Jiang-Hua Liu, Qilin Yu, Xin Wen, and Yu Liu*

Dedicated to the 100th anniversary of Nankai University

Abstract: Tunable protein assemblies not only hold a dominant position in vital biological events but are also a significant theme in supramolecular chemistry. Herein, we demonstrated that the intertubular aggregation of microtubules (MTs) could be efficiently regulated by a synergistic polypeptide–tubulin interaction and host–guest complexation. The benzyliimidazolium-modified antimetabolic peptide (BP) could recognize the MTs and concurrently form stable inclusion complexes with avirulent cucurbit[7]uril (CB[7]) and cucurbit[8]uril (CB[8]) in different binding stoichiometries. The self-assembling morphology of MTs was converted from fibrous to nanoparticulate aggregates via extensive BP⊂CB[8] cross-linkage, leading to significant cell apoptosis and tumor ablation *in vivo*. The targeted (BP⊂CB[8])@MT ternary assembly provides a facile supramolecular method to enhance the protein–protein interactions, which may be developed as a therapy for degenerative diseases, such as cancer.

Supramolecular methodology based on the cavity-bearing synthetic macrocycles (for example, cyclodextrin, calixarene, cucurbituril, pillararene, and others) has proven a powerful strategy to mimic and regulate the structures and functions of many naturally occurring biomacromolecules, such as nucleic acids and proteins.^[1] In particular, the incorporation of molecular binding sites that can be specifically recognized by macrocyclic receptors can be developed as an effective means to modulate of protein–protein interactions. Thus, the diversity and complexity of macrocycle–protein supramolecular entities have stimulated emerging opportunities and tremendous potential in miscellaneous fields, such as controlled energy transfer, bio-catalysis/sensing, morphological interconversion, and cell-viability regulation.^[2]

Microtubules (MTs), key protein filaments of the cytoskeleton, are constructed by the regular arrangement of globular α/β -tubulin heterodimers in a highly dynamic manner.^[3] The polymerization and depolymerization of MTs

have critical relevance to cell division and intracellular transport, which make these inter-networked tubular arrays attractive molecular targets for cancer chemotherapy^[4] and biomolecular assemblies.^[5] Further to some known natural-product MT stabilizing/destabilizing agents (for example, paclitaxel and vinca alkaloids),^[6] tubulin-targeted antimetabolic peptides have become alternative or even prime candidates for innovative drug discovery and development, mainly due to their immense advantages in avoiding the general cytotoxicity and multidrug resistance of conventional chemotherapeutic compounds.^[7,8]

The design of our system was based on the inspection of a selected polypeptide containing ten amino acids, which was identified by computational analysis and exhibited antimetabolic activity by competitive binding with the α -tubulin subunit.^[9] To further explore the curative effect of supramolecular intertubular aggregation, we present an entirely self-assembled microtubular system, which is fabricated by the combination of primary tubulin–tubulin heterodimerization, specific peptide–tubulin recognition, and cooperative host–guest complexation. In our case, the chemical modification of a benzyliimidazolium moiety with an antimetabolic polypeptide (BP) did not interfere with its original tubulin-targeting ability, but it provided a functional anchoring point to noncovalently interact with cucurbiturils (CB[7] and CB[8]). Moreover, the 2:1 homoternary BP⊂CB[8] complexation with MTs could exclusively induce the dramatic morphological change of MTs from linear polymers to spherical nanostructures. Significantly, a highly efficacious anticancer potency was achieved after treatment with BP⊂CB[8] complex, as evidenced by more compact MTs in the cellular environment and higher levels of apoptosis in the tumor tissues. Thus, it appears that the enhanced intertubular aggregation arising from the precise and orthogonal supramolecular motifs can be exploited as a novel strategy in the battle against MT-aggregation-related diseases.

The construction of the (BP⊂CB[8])@MT supramolecular assembly is depicted in Figure 1. The synthetic route and compound characterization of the guest peptide BP are shown in the Supporting Information (Supporting Information, Figures S1–S10). In our case, the 1-benzyliimidazolium group was covalently bonded to the tubulin-targeted antimetabolic peptide at its N-terminus via an extra linkage containing acylmethylene and alanine residues. These biologically nonessential segments with appropriate molecular length could facilitate the complete 1:2 homoternary complexation of CB[8] with the benzyliimidazolium moiety of the

[*] Dr. Y.-M. Zhang, J.-H. Liu, Dr. Q. Yu, Dr. X. Wen, Prof. Y. Liu
College of Chemistry,
State Key Laboratory of Elemento-Organic Chemistry,
Nankai University, Tianjin 300071 (China)
E-mail: yuliu@nankai.edu.cn

Dr. X. Wen
Department of Chemical Biology,
National Pesticide Engineering Research Center,
Nankai University, Tianjin 300071 (China)

 Supporting information and the ORCID identification number(s) for the author(s) of this article can be found under:
 <https://doi.org/10.1002/anie.201903243>

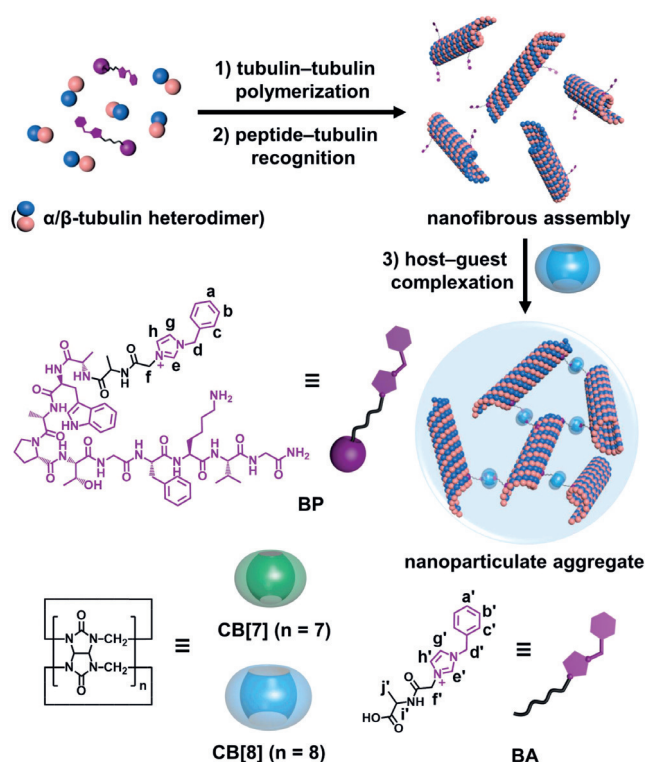


Figure 1. Schematic illustration of (BP \subset CB[8])@MT ternary supramolecular assembly for targeted microtubular aggregation.

BP peptide and simultaneously ensure the specific peptide-tubulin interaction.

The host-guest binding behaviors were preliminarily explored by ^1H NMR spectroscopy. As discerned from Figure 2, the proton signals of benzyl ($\text{H}_{\text{a-d}}$) and imidazolium (H_{e}) groups in the guest peptide BP exhibited pronounced upfield shifts, while the proton signal of the methylene group in the acylmethylene linker (H_{f}) shifted downfield upon complexation with CB[7] and CB[8]. In contrast, the resonance signals of the polypeptide chain were almost unchanged upon addition of CB[7] and CB[8] (dashed box in Figure 2). These complexation-induced chemical-shift changes were further elucidated using the carboxylated precursor (BA, Figure 1) as a reference compound. These chemical-shift changes resembled those of observed when using BP (Supporting Information, Figure S11). These results demonstrate that the benzylimidazolium moiety was exclusively included in the cavity of CB via favorable ion-dipole interaction between the positively charged imidazole salts and the portal oxygen atoms of CB, leaving the polypeptide chain outside the cavity.^[10]

Furthermore, the complexation stoichiometries and binding constants (K_{S}) were explored using ^1H NMR and microcalorimetric titration experiments, respectively. As shown in Figures S12 and S13 in the Supporting Information, fast exchange equilibria were observed in the molecular recognition between CB[7] and the benzylimidazolium-bearing guest molecules. Moreover, the K_{S} values were calculated as $(7.46 \pm 0.57) \times 10^5$ and $(8.66 \pm 0.43) \times 10^5 \text{ M}^{-1}$ upon complexation of CB[7] with BA and BP, respectively, by means of

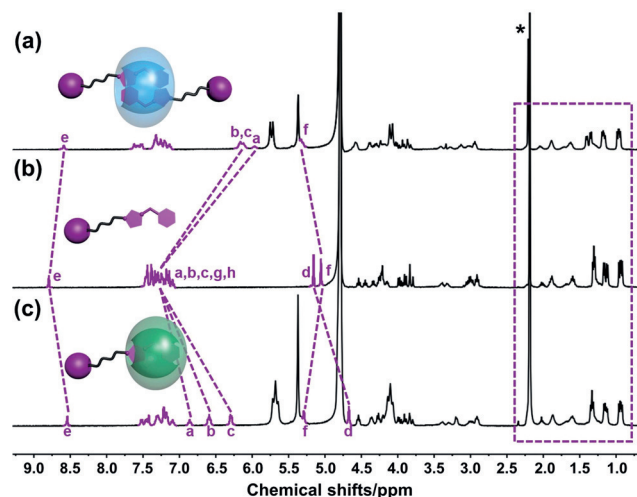


Figure 2. Partial ^1H NMR spectra (400 MHz, D_2O , 25°C) of a) BP \subset CB[8] complex, b) free BP, and c) BP \subset CB[7] complex ([BP] = [CB-7]) = 1.5 mM and [CB[8]] = 0.75 mM). The asterisk indicates 0.5% acetone as an internal standard at 2.22 ppm in D_2O .

isothermal titration calorimetry (ITC) based on a 1:1 complex stoichiometry (Supporting Information, Figures S14 and S15). In contrast, both free and bound guest molecules could be clearly distinguished on the ^1H NMR time scale, due to the slow exchange equilibria in the molecular recognition processes involving CB[8].^[11] Moreover, the chemical shifts of H_{e} on BP and $\text{H}_{\text{e}'}$ on BA versus the molar ratio show an inflection point at a molar ratio of 0.5, corresponding to a 2:1 host-guest binding stoichiometry with CB[8] (Supporting Information, Figures S16–S19). Accordingly, ITC measurements afforded K_{S} values as high as $(4.20 \pm 0.06) \times 10^{11}$ and $(5.15 \pm 0.04) \times 10^{11} \text{ M}^{-2}$ for BA \subset CB[8] and BP \subset CB[8] complexes, respectively, suggesting an extraordinarily strong binding affinity of CB[8] with the benzylimidazolium unit (Supporting Information, Figures S20 and S21). These quite similar binding strengths once again corroborate that the introduction of a tubulin-targeted peptide chain did not negatively impact the molecular binding behaviors between CB[8] and benzylimidazolium units. Furthermore, complete encapsulation of BP in CB[8] was also observed under physiological buffer solution (in D_2O containing 150 mM NaCl at 37°C , Supporting Information, Figure S22).

Subsequently, the influence of 1:1 complexation with CB[7] and 2:1 supramolecular cross-linkage with CB[8] on microtubular aggregation behaviors was characterized by transmission electron microscopy (TEM). As can be seen in Figure 3a, free MT exhibited uniform fibrous nanostructures of several hundred nanometers in length, suggesting the spontaneous formation of MTs by $\alpha</math>/ $\beta</math>-tubulin heterodimers in general tubulin buffer solution. Meanwhile, the addition of tubulin-targeted peptide at a relatively lower concentration could not affect the microtubular assembly (Figure 3b). Surprisingly, nanoparticulate assemblies were clearly observed with an average diameter of 700 nm in the case of (BP \subset CB[8])@MT, which was attributed to intertubular aggregation via BP \subset CB[8] complexation (Figure 3c). In the control experiments, the fibrous morphology of MTs was$$

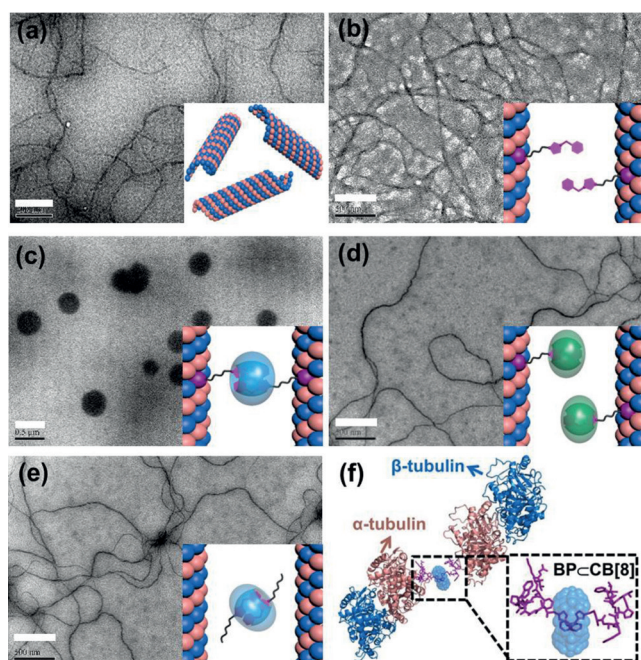


Figure 3. TEM images of a) free MTs, b) BP@MTs, c) (BP \subset CB[8])@MTs, d) (BP \subset CB[7])@MTs, e) mixture of MTs and BA \subset CB[8] complex (initial concentration: [tubulin] = 1.0 mg mL⁻¹, [BP] = [BA] = [CB[7]] = 50 μ M, [CB[8]] = 25 μ M, pH 6.8). The scale bar in each TEM image is 500 nm. f) Schematic illustration of BP \subset CB[8] complex with α - and β -heterodimeric tubulins. The BP peptide is shown in purple.

largely maintained in the presence of free CB[7], CB[8], BP \subset CB[7] or BA \subset CB[8] complex (Figure 3 d,e and Supporting Information, Figure S23). These results show that the single polypeptide–tubulin interaction or the formation of inclusion complexes is not sufficient to change the microtubule assembly and the CB[8]-assisted multivalent supramolecular cross-linkage is an indispensable factor in inducing morphological conversion during microtubular aggregation. The schematic illustration in conjunction with the docking study on the formation of an inclusion complex with CB[8] is shown in Figure 3 f, suggesting that the bridging of two α/β -tubulin dimers could be achieved by 2:1 BP \subset CB[8] complexation (Supporting Information).

Along with the TEM results, there was an obvious size change in aqueous media. The optical transmittance sharply decreased and the broadened hydrodynamic diameter distribution instantly appeared in the large-size region upon addition of CB[8] to the solution of BP–tubulins, whereas no significant change was observed for individual, BP-decorated MTs, or MT/CBs mixtures by dynamic light scattering or UV transmittance experiments (Supporting Information, Figures S24 and S25). Furthermore, clear signals assigned to the formation of aggregates were also observed when using different concentrations of BP \subset CB[8] complex. These results indicate the formation of large-sized intertubular nanoaggregates resulting from the complexation of multiple BP \subset CB[8] by MTs in buffer solution. Overall, combining results of the ¹H NMR spectral examination and the morphological variations in the microtubular aggregation

process, it is anticipated that the orthogonal host–guest and polypeptide–tubulin interactions in the (BP \subset CB[8])@MT supramolecular system would strongly affect the concomitant biological performance of MTs.

Confocal laser scanning microscopy was employed to investigate the complexation-induced intertubular aggregation in human lung adenocarcinoma (A549) cells. Initially, MTs labeled with rhodamine-labeled BP were uniformly distributed around/in the nucleus, which was in good colocalization with the MTs labeled with fluorescein isothiocyanate (FITC)-tagged antibody. Spherically aggregated MTs were clearly observed in the selected cell line after treatment with CB[8] (Figure 4 a and Supporting Information, Figure S26). The cell viability slightly changed after incubation with BP alone for 24 h, whereas the BP \subset CB[8] complexes exhibited remarkable dose-dependent cytotoxicity under the same experimental conditions. Taking the BP concentration at 320 μ M as an example, the relative cell viability sharply decline from 81 % to 43 % in the presence of essentially nontoxic CB[8] (Figure 4 b). Meanwhile, the propidium iodide (PI) staining experiments further verified that the co-incubation of BP-treated cells with CB[8] gave a substantial increase in the percentage of dead cells in the wide concen-

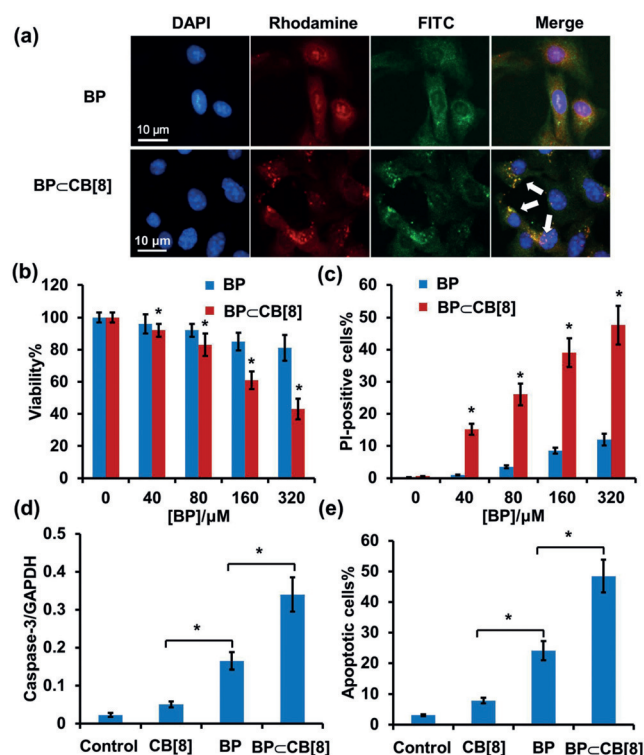


Figure 4. In vitro suppression of cellular proliferation by BP \subset CB[8] complexation with MTs. a) Confocal fluorescence images of A549 cells incubated with BP \subset CB[8] complex. Rhodamine-labeled BP (red) and FITC-tagged antibody (green) were used to stain the MT skeleton and DAPI (4',6-diamidino-2-phenylindole, blue) was used to stain nucleus. The typical condensed MTs are indicated by white arrows. Changes in b) cell viability, c) level of PI-positive cells, d) ratio of cleaved caspase-3 to GAPDH, and e) level of apoptotic cells by BP \subset CB[8] complexation with MTs. Asterisks in (b–e) indicate the statistically significant differences among groups (* p < 0.05).

tration range of 40–320 μM (Figure 4c). In the control experiments, the cell viability and the percentage of PI-positive cells were almost unchanged upon addition of BP \subset CB[7] complex, further confirming the vital importance of supramolecular intertubular aggregation by BP \subset CB[8] complexation (Supporting Information, Figure S27). Moreover, the expression of the apoptosis-related protease, caspase-3, was also evaluated using glyceraldehyde phosphate dehydrogenase (GAPDH) as internal reference (Figure 4d). Compared to untreated and CB[8]-treated cells, the complexation of BP with CB[8] lead to a prominent increase in caspase-3 levels, indicative of a significant induction of cell apoptosis. The number of apoptotic cells also dramatically elevated in the presence of BP \subset CB[8] complex (Figure 4e). Accordingly, the half-maximal inhibitory concentration (IC_{50}) of the BP \subset CB[8] complex was calculated as $238.7 \pm 52.5 \mu\text{M}$, whereas BP alone showed no significant cytotoxic activity at the tested concentrations. These results suggest that the CB[8]-mediated multivalent cross-linkage can seriously interfere with MT assembly in living cancer cells and eventually cause cell death mainly through a caspase-dependent pathway.

Finally, given the complexation-induced intertubular aggregation and the enhanced apoptosis in the cellular environment, the anticancer potency of BP \subset CB[8] complexation was further evaluated in a tumor-burdened mouse mode. As expected, among all of the examined groups, the tumor volume and weight decreased after treatment with BP \subset CB[8] complex over the entire experimental period (Figure 5a–b and Supporting Information, Figure S28). Moreover, the terminal deoxynucleotidyl transferase dUTP nick end labeling (TUNEL) assay of tumors showed a much stronger green fluorescence emission in the BP \subset CB[8]-treated group, corresponding to fluorescein-stained DNA fragmentation in these apoptotic cells (Figure 5c). Quantitative analysis also revealed a higher population of TUNEL-positive cells (around 44%) in the BP \subset CB[8]-treated tumor tissues, which further confirmed the importance of CB[8]-mediated supramolecular complexation in inducing significant cell apoptosis in vivo (Figure 5d). Taken together, the administration of BP \subset CB[8] complex carrying tubulin-targeted antimetabolic peptides was proven to be the most effective formulation in inducing apoptosis and suppressing tumor growth.

In conclusion, the antimetabolic peptide BP was modified with a benzylimidazolium moiety, facilitating its noncovalent encapsulation by CB[7] and CB[8] while still retaining its tubulin-targeting ability. As investigated by morphological characterization, the intertubular aggregation of MTs could be efficiently regulated via BP \subset CB[8] complexation. Moreover, through in vitro and in vivo evaluation, extensive supramolecular MT cross-linking can induce significant cell apoptosis, ultimately resulting in the suppression of tumor proliferation. This work emphasizes the immense advantage of a combinatorial strategy that involves a biocompatible tubulin-targeting agent and controlled supramolecular complexation in the (BP \subset CB[8])@MT assembly, which can be developed as a therapeutic method for cancer treatment. We also envision that, equipped with other specific cell/tissue-targeting groups, our approach based on targeted and

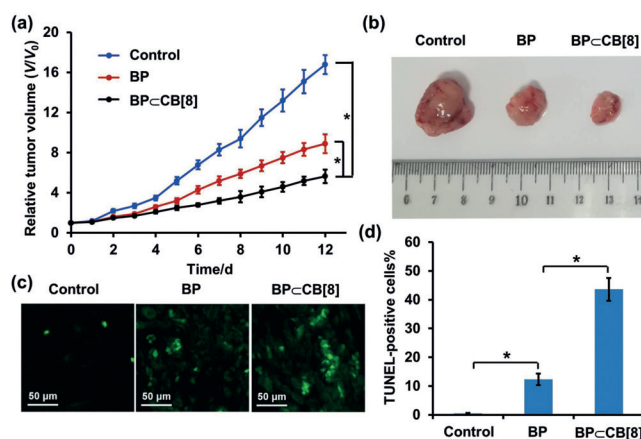


Figure 5. In vivo inhibition of tumor growth for BALB/c mice bearing S180 cancer cells treated with blank control (PBS), BP, and BP \subset CB[8] complex. a) Time-dependent changes in the relative tumor volume after different treatments ($n = 6$, mean \pm s.d.); b) representative photograph of tumors at the end of the anticancer experiments; c) confocal fluorescence images of TUNEL assay of tumor tissues. DNA fragments in apoptotic cells were stained with fluorescein-conjugated deoxynucleotide (green); d) ratio of TUNEL-positive cells:total cells. Asterisks in (a) and (d) indicate the statistically significant differences among groups ($*p < 0.05$). The injected dose was normalized to $0.06 \text{ mmol kg}^{-1}$ BP.

controlled protein–protein interactions may open up new opportunities for clinical translation of supramolecular therapeutics.

Acknowledgements

This work was financially funded by the NNSFC (grants 21432004, 21871154, 21772099, and 21861132001).

Conflict of interest

The authors declare no conflict of interest.

Keywords: apoptosis · cucurbituril · host–guest chemistry · microtubular aggregation · supramolecular chemistry

How to cite: *Angew. Chem. Int. Ed.* **2019**, *58*, 10553–10557
Angew. Chem. **2019**, *131*, 10663–10667

- [1] a) Y.-W. Yang, Y.-L. Sun, N. Song, *Acc. Chem. Res.* **2014**, *47*, 1950–1960; b) M. Giuliani, I. Morbioli, F. Sansone, A. Casnati, *Chem. Commun.* **2015**, *51*, 14140–14159; c) Q. Luo, C. Hou, Y. Bai, R. Wang, J. Liu, *Chem. Rev.* **2016**, *116*, 13571–13632; d) S. van Dun, C. Ottmann, L.-G. Milroy, L. Brunsveldt, *J. Am. Chem. Soc.* **2017**, *139*, 13960–13968; e) C. Hou, Z. Huang, Y. Fang, J. Liu, *Org. Biomol. Chem.* **2017**, *15*, 4272–4281; f) H. Kitagishi, S. Minegishi, *Chem. Pharm. Bull.* **2017**, *65*, 336–340; g) L. Kuan, F. R. G. Bergamini, T. Weil, *Chem. Soc. Rev.* **2018**, *47*, 9069–9105; h) Y. Wang, X. Zhang, G. Zou, S. Peng, C. Liu, X. Zhou, *Acc. Chem. Res.* **2019**, <https://doi.org/10.1021/acs.accounts.8b00543>.
- [2] a) J. M. Chinai, A. B. Taylor, L. M. Ryno, N. D. Hargreaves, C. A. Morris, P. J. Hart, A. R. Urbach, *J. Am. Chem. Soc.* **2011**,

- 133, 8810–8813; b) D. T. Dang, H. D. Nguyen, M. Merckx, L. Brunsveld, *Angew. Chem. Int. Ed.* **2013**, *52*, 2915–2919; *Angew. Chem.* **2013**, *125*, 2987–2991; c) H. H. Lee, T. S. Choi, S. J. Lee, J. W. Lee, J. Park, Y. H. Ko, W. J. Kim, K. Kim, H. I. Kim, *Angew. Chem. Int. Ed.* **2014**, *53*, 7461–7465; *Angew. Chem.* **2014**, *126*, 7591–7595; d) R. P. Bosmans, J. M. Briels, L. G. Milroy, T. F. de Greef, M. Merckx, L. Brunsveld, *Angew. Chem. Int. Ed.* **2016**, *55*, 8899–8903; *Angew. Chem.* **2016**, *128*, 9045–9049; e) P. J. de Vink, J. M. Briels, T. Schrader, L. G. Milroy, L. Brunsveld, C. Ottmann, *Angew. Chem. Int. Ed.* **2017**, *56*, 8998–9002; *Angew. Chem.* **2017**, *129*, 9126–9130; f) F. Guagnini, P. M. Antonik, M. L. Rennie, P. O'Byrne, A. R. Khan, R. Pinalli, E. Dalcanale, P. B. Crowley, *Angew. Chem. Int. Ed.* **2018**, *57*, 7126–7130; *Angew. Chem.* **2018**, *130*, 7244–7248; g) Y.-M. Zhang, N.-Y. Zhang, K. Xiao, Q. Yu, Y. Liu, *Angew. Chem. Int. Ed.* **2018**, *57*, 8649–8653; *Angew. Chem.* **2018**, *130*, 8785–8789; h) M. L. Rennie, G. C. Fox, J. Perez, P. B. Crowley, *Angew. Chem. Int. Ed.* **2018**, *57*, 13764–13769; *Angew. Chem.* **2018**, *130*, 13960–13965.
- [3] a) K. C. Nicolaou, F. Roschangar, D. Vourloumis, *Angew. Chem. Int. Ed.* **1998**, *37*, 2014–2045; *Angew. Chem.* **1998**, *110*, 2120–2153; b) G. J. Brouhard, L. M. Rice, *Nat. Rev. Mol. Cell Biol.* **2018**, *19*, 451–463.
- [4] C. Dumontet, M. A. Jordan, *Nat. Rev. Drug Discovery* **2010**, *9*, 790–803.
- [5] a) G. D. Bachand, E. D. Spoerke, M. J. Stevens, *Biotechnol. Bioeng.* **2015**, *112*, 1065–1073; b) R. Mogaki, P. K. Hashim, K. Okuro, T. Aida, *Chem. Soc. Rev.* **2017**, *46*, 6480–6491.
- [6] a) Y.-N. Cao, L. L. Zheng, D. Wang, X. X. Liang, F. Gao, X. L. Zhou, *Eur. J. Med. Chem.* **2018**, *143*, 806–828; b) D. Bates, A. Eastman, *Br. J. Clin. Pharmacol.* **2017**, *83*, 255–268.
- [7] a) E. Hamel, *Biopolymers* **2002**, *66*, 142–160; b) A. T. Fojo, M. Menefee, *Semin. Oncol.* **2005**, *32*, S3–S8; c) J. R. Jackson, D. R. Patrick, M. M. Dar, P. S. Huang, *Nat. Rev. Cancer* **2007**, *7*, 107–117; d) M. Kavallaris, *Nat. Rev. Cancer* **2010**, *10*, 194–204.
- [8] a) S. Mohapatra, A. Saha, P. Mondal, B. Jana, S. Ghosh, A. Biswas, S. Ghosh, *Adv. Healthcare Mater.* **2017**, *6*, 1600718; b) J. Stöhr, H. Wu, M. Nick, Y. Wu, M. Bhate, C. Condello, N. Johnson, J. Rodgers, T. Lemmin, S. Acharya, J. Becker, K. Robinson, M. J. S. Kelly, F. Gai, G. Stubbs, S. B. Prusiner, W. F. DeGrado, *Nat. Chem.* **2017**, *9*, 874–881; c) B. Jana, P. Mondal, A. Saha, A. Adak, G. Das, S. Mohapatra, P. Kurkute, S. Ghosh, *Langmuir* **2018**, *34*, 1123–1132; d) H. Kadavath, Y. Cabrales Fontela, M. Jaremko, L. Jaremko, K. Overkamp, J. Biernat, E. Mandelkow, M. Zweckstetter, *Angew. Chem. Int. Ed.* **2018**, *57*, 3246–3250; *Angew. Chem.* **2018**, *130*, 3301–3305.
- [9] S. Pieraccini, G. Saladino, G. Cappelletti, D. Cartelli, P. Francescato, G. Speranza, P. Manitto, M. Sironi, *Nat. Chem.* **2009**, *1*, 642–648.
- [10] a) D. Jiao, F. Biedermann, F. Tian, O. A. Scherman, *J. Am. Chem. Soc.* **2010**, *132*, 15734–15743; b) J. Liu, C. S. Tan, Z. Yu, N. Li, C. Abell, O. A. Scherman, *Adv. Mater.* **2017**, *29*, 1605325.
- [11] a) S. J. Barrow, S. Kasera, M. J. Rowland, J. D. Barrio, O. A. Scherman, *Chem. Rev.* **2015**, *115*, 12320–12406; b) H. Zou, J. Liu, Y. Li, X. Li, X. Wang, *Small* **2018**, *14*, 1802234; c) E. Pazos, P. Novo, C. Peinador, A. E. Kaifer, M. D. Garcia, *Angew. Chem. Int. Ed.* **2019**, *58*, 403–416; *Angew. Chem.* **2019**, *131*, 409–422.

Manuscript received: March 15, 2019
Revised manuscript received: June 4, 2019
Accepted manuscript online: June 4, 2019
Version of record online: June 27, 2019